Science of the Total Environment 912 (2024) 169055

Contents lists available at ScienceDirect

Science of the Total Environment

journal homepage: www.elsevier.com/locate/scitotenv

High-time resolution $PM_{2.5}$ source apportionment assisted by spectrum-based characteristics analysis

Jie Liu [a,c], Fangjingxin Ma [a], Tse-Lun Chen [c,d], Dexun Jiang [b,c], Meng Du [a], Xiaole Zhang [e], Xiaoxiao Feng [c,d], Qiyuan Wang [f], Junji Cao [f], Jing Wang [c,d,*]

[a] School of Water Conservancy & Civil Engineering, Northeast Agricultural University, Harbin 150030, China
[b] School of Information Engineering, Harbin University, Harbin 150086, China
[c] Institute of Environmental Engineering (IfU), ETH Zürich, 8093 Zürich, Switzerland
[d] Laboratories of Advanced Analytical Technologies, Swiss Federal Laboratories for Materials Science and Technology, 8600 Dübendorf, Switzerland
[e] Institute of Public Safety Research, Department of Engineering Physics, Tsinghua University, Beijing 100084, China
[f] Key Laboratory of Aerosol Chemistry and Physics, State Key Laboratory of Loess and Quaternary Geology, Institute of Earth Environment, Chinese Academy of Sciences, Xi'an, China

HIGHLIGHTS

- Frequency spectrum characteristics are extracted for anomaly identification.
- Anomaly frequency, location, duration and intensity can be captured.
- The spectrum-based source apportionment solution of $PM_{2.5}$ pollution is obtained.
- Spectrum characteristics can provide explanations for source information.
- Spectral analyses can assist PMF for reliable source apportionment solution.

GRAPHICAL ABSTRACT

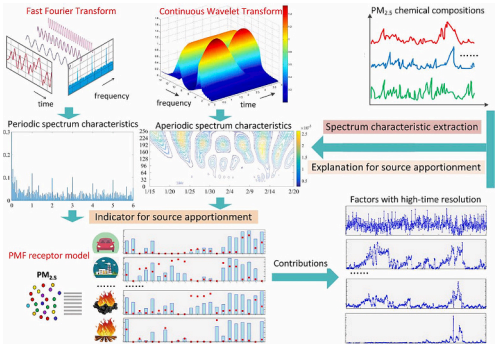

ARTICLE INFO

Editor: Kai Zhang

Keywords:
$PM_{2.5}$ pollution
Spectrum characteristics extraction
Source apportionment
High-time resolution
Spectral analysis

ABSTRACT

Characteristics extraction and anomaly analysis based on frequency spectrum can provide crucial support for source apportionment of $PM_{2.5}$ pollution. In this study, an effective source apportionment framework combining the Fast Fourier Transform (FFT)- and Continuous Wavelet Transform (CWT)-based spectral analyses and Positive Matrix Factorization (PMF) receptor model is developed for spectrum characteristics extraction and source contribution assessment. The developed framework is applied to Beijing during the winter heating period with 1-h time resolution. The spectrum characteristics of anomaly frequency, location, duration and intensity of $PM_{2.5}$ pollution can be captured to gain an in-depth understanding of source-oriented information and provide necessary indicators for reliable PMF source apportionment. The combined analysis demonstrates that the secondary inorganic aerosols make relatively high contributions (50.59 %) to $PM_{2.5}$ pollution during the winter heating period in Beijing, followed by biomass burning, vehicle emission, coal combustion, road dust, industrial process and firework emission sources accounting for 15.01 %, 11.00 %, 10.70 %, 5.31 %, 3.88 %, and 3.51 %,

* Corresponding author at: Institute of Environmental Engineering (IfU), ETH Zürich, 8093 Zürich, Switzerland.
E-mail address: jing.wang@ifu.baug.ethz.ch (J. Wang).

https://doi.org/10.1016/j.scitotenv.2023.169055
Received 15 June 2023; Received in revised form 14 November 2023; Accepted 30 November 2023
Available online 5 December 2023

respectively. The source apportionment result suggests that combining frequency spectrum characteristics with source apportionment can provide consistent rationales for understanding the temporal evolution of $PM_{2.5}$ pollution, identifying the potential source types and quantifying the related contributions.

1. Introduction

In recent years, China is persistently suffering from serious haze episodes along with the rapid economic growth and excessive human activities (Lv et al., 2021; Park et al., 2022). The haze episodes have negative influences on climate changes owing to the absorption and scattering of solar radiation, as well as human health due to prolonged exposure to the associated pollutions (Almeida et al., 2020; Chen et al., 2022). The fine particulate matter ($PM_{2.5}$) acts as a key inducement of haze episodes and originates from multiple anthropogenic sources (Tao et al., 2017; Kim et al., 2018; Chen et al., 2023). It is crucial to identify the chemical composition characteristics and reveal the source-oriented information from potential multiple sources of $PM_{2.5}$ pollution for a comprehensive source apportionment (Balachandran et al., 2013; Alias et al., 2020). With the development of data-driven technologies and accumulation of high-time resolution observations, the receptor-based source apportionment method associated with substantial source-oriented spectrum information can provide reasonable source characteristics and facilitate understanding of their contributions for atmospheric pollution monitoring and control (Stanek et al., 2011; Yu et al., 2019).

Receptor-based models have recently attracted considerable attentions, and have become prevalent in the field of source apportionment of $PM_{2.5}$ pollution (Crilley et al., 2017; Taghvaee et al., 2018; Almeida et al., 2020). Positive Matrix Factorization (PMF), as a receptor-based source apportionment tool, can provide quantitative contribution information without prior knowledge of sources, especially using high-time resolution measurements of $PM_{2.5}$ chemical components (Yu et al., 2019; Bland et al., 2022), which has been widely applied to multiple Chinese urban regions (Lei et al., 2019; Yu et al., 2019; Rai et al., 2021; Lv et al., 2021) and other countries (Masiol et al., 2017; Park et al., 2019; Tobler et al., 2020; Veld et al., 2021; Manousakas et al., 2022). The high-time resolution observations of $PM_{2.5}$ chemical components can provide more robust PMF source apportionment results as they can help PMF obtain a well-defined relationship between the driving factors and sources even if using short-period time-varying signals (Vedantham et al., 2014; Feng et al., 2016; Zhang et al., 2023a). However, the inherent uncertainty and complexity of atmospheric environmental systems make it difficult to identify the driving factors contributing to haze episodes and associated source information (Srivastava et al., 2021). Therefore, the PMF source apportionment of $PM_{2.5}$ pollution under time-domain patterns faces strong challenges.

Source-oriented frequency features can be extracted by analyzing the spectrum characteristics corresponding to the $PM_{2.5}$ chemical components. These frequency-domain features can provide inherent information about the emission patterns and anomaly levels of the potential sources, and help effectively distinguish the various source types and contributions. Thus, incorporating spectrum information into PMF source apportionment can be a valuable approach to enhance the understanding of $PM_{2.5}$ pollution sources. The relationships between $PM_{2.5}$ chemical components and source characteristics are usually determined by various factors and complex interactions. It is necessary to reasonably retrieve the complex relationships based on the extracted spectrum information of $PM_{2.5}$ pollution under frequency-domain patterns (Chi and Lin, 2021). Generally, spectral analyses, as signal process technologies, including the Fourier transform and wavelet analysis (Rai and Mohanty, 2007; Li et al., 2013), can analyze the periodic and aperiodic features of the original time-varying signals for feature extraction (Jiang et al., 2020). Fast Fourier Transform (FFT) algorithm is generally used to transfer the original time-varying signals of $PM_{2.5}$ chemical components from the time domain to the frequency domain for the related periodic feature extraction. Since it assumes that the frequency information of the original signals does not change with time, FFT is unable to capture transient variations of non-stationary signals occurring at a specific time. In contrast, Continuous Wavelet Transform (CWT) algorithm, which performs well in capturing the localization variation features of non-stationary signals, can analyze the relationship between the time domain and frequency domain, and thereby efficiently identify regional anomaly features (Chen et al., 2020; Ma et al., 2022). Barmpadimos et al. (2011) used FFT algorithm to examine the periodic patterns using time-varying signals of PM_{10} and $PM_{2.5}$ concentrations; Yu et al. (2022) adopted FFT algorithm to extract the periodic features of $PM_{2.5}$ and assessed spatial-temporal heterogeneity; Chen et al. (2020) applied CWT algorithm to extract useful localization features for understanding the temporal evolution characteristics of $PM_{2.5}$ pollution; Li et al. (2021) identified the anomaly features based on CWT algorithm for multi-scale evaluation of $PM_{2.5}$ pollution. The frequency spectrum information can enhance our understanding of the source types in PMF, exhibit a clearer link between factors and sources, and provide explanatory evidence for potential source information of $PM_{2.5}$ pollution. However, existing studies have estimated pollution source types and their contributions by receptor models only based on temporal variation from the time domain, neglecting spectrum information from the frequency domain (Chen et al., 2020; Ma et al., 2022). In order to comprehensively understand and explain the source information of $PM_{2.5}$ pollution, it is necessary to develop a hybrid source apportionment framework incorporating the spectrum characteristics in addition to the temporal variations.

Therefore, the objective of this study is to develop a hybrid source apportionment framework combining the spectral analysis and receptor model to capture the periodic and aperiodic spectrum characteristics, identify the potential source types and quantify their contributions for spectrum-based source apportionment of $PM_{2.5}$ pollution. The FFT- and CWT-based spectral analyses are used to extract periodic and aperiodic spectrum characteristics of $PM_{2.5}$ pollution. The PMF-based receptor model is used to analyze the potential source types and their contributions assisted by the spectrum characteristics. The developed framework is then applied to Beijing in China to analyze the related source contributions based on spectrum characteristics during the winter heating period. The developed framework could be a promising pathway to harmonize the spectral analysis and receptor model for a comprehensive source apportionment. And the spectrum-based source apportionment results could demonstrate a new understanding of the relationship between emission sources and $PM_{2.5}$ pollution.

2. Material and methods

2.1. Sampling site and data collection

2.1.1. Sampling site

The sampling site at the Institute of Atmospheric Physics (IAP) of the Chinese Academy of Sciences (116.39° E, 39.98° N), located in the Chaoyang District in the northeast of Beijing representing a typical urban location, is selected to demonstrate the developed source apportionment framework shown in Fig. S1. The measurements of the related $PM_{2.5}$ elements, which span from 7:00 am on January 15, 2021 to 6:00 am on February 20, 2021, were collected with 1-h time resolution during the winter heating period.

2.1.2. Chemical analysis

The water-soluble ions of $PM_{2.5}$ sample, including nitrate (NO_3^-),

sulfate (SO_4^{2-}), ammonium (NH_4^+), and chloride (Cl^-), were analyzed by Quadrupole Aerosol Chemical Speciation Monitor (Q-ACSM, Aerodyne Research Inc., Billerica, Massachusetts, USA). The metallic elements, including Si, K, Ca, V, Cr, Mn, Fe, Co, Ni, Cu, Zn, Ga, As, Se, Pd, Ag, Cd, Sn, Sb, Ba, Hg, Tl, and Pb, were measured by Xact 625i Ambient Metals Monitor (X625i, Cooper Environmental Services, Beaverton, OR, USA). The black carbon (BC) component was measured by Aethalometer (AE33, Magee Scientific, Berkeley, CA, USA). A more detailed information about the calibration methods of the monitoring instruments can be found in Section 1 of the Supporting Information. In addition, the concentrations of $PM_{2.5}$ and other gaseous pollutants, such as CO, SO_2, NO_2, and O_3 were also collected with 1-h time resolution at the Olympic Sports Center station (116.41° E, 39.99° N, Chaoyang District, 2.04 km from the sampling site) during the same sampling period using the gas analyzers. The meteorological data, including air temperature (AT), relative humidity (RH), and wind speed rate (WSR) were measured at Beijing Capital International Airport station (116.60° E, 40.08° N, Chaoyang District, 21.08 km from the sampling site). A more detailed information about the geographical location of sampling site can be found in Section 2 of the Supporting Information.

2.1.3. Mass concentration of OC and EC

The absorption signal at near-infrared range (880 nm) is adopted to calculate the concentrations of BC mass (Lei et al., 2019). The concentrations of elemental carbon (EC) mass can be assumed to be equivalent to the concentrations of BC mass (Hsiao et al., 2021). Meanwhile, the absorption signal at near-UV range (370 nm) is regarded as ultraviolet particulate matter (UVPM). The difference between UVPM and BC is denoted as △C, which can be calculated as follows (Liu et al., 2020; Chang et al., 2022):

$$\triangle C = \mathrm{UVPM} - \mathrm{BC} \tag{1}$$

Generally, the concentrations of organic carbon (OC) mass can be assumed to be equivalent to △C (Olson et al., 2015).

2.2. Spectrum-based analysis for anomaly feature extraction

2.2.1. FFT algorithm for periodic characteristics analysis

FFT algorithm can decompose the different components contained in the original discrete signals into the sum of countless sinusoidal signals with different frequencies. For the original discrete signals $f(n)$, the spectrum information of the original signals $F(k)$ can be expressed as follows (Cooley and Tukey, 1965):

$$F(k) = \sum_{n=0}^{N-1} f(n) \cdot e^{-i2\pi kn/N} \quad (k = 0,\ 1,\ 2,\ \ldots,\ N-1) \tag{2}$$

where n is the size of the data samples; $e^{i2\pi/N}$ is a primitive Nth root of 1. FFT algorithm can ensure a fast calculation speed by reducing the complexity from $O(n^2)$ to $O(nlogn)$ for a computation process with size n (Rajaby and Sayedi, 2022).

2.2.2. CWT algorithm for aperiodic characteristics analysis

CWT algorithm compares the original time-varying signals $f(t)$ to the wavelet at various scales, which can be obtained as follows (Munoz et al., 2002; Tary et al., 2018):

$$C(a,\ b,\ f(t)\ ,\ \psi(t)\ ) = \int_{-\infty}^{\infty} f(t) \frac{1}{a} \psi^* \left(\frac{t-b}{a} \right) dt \tag{3}$$

where a is the scale parameter ($a > 0$), and b is the position parameter of a reference wavelet ψ. ψ^* denotes the complex conjugate of the reference wavelet. By continuously varying the values of the scale parameter a and the position parameter b, the wavelet coefficients $C(a,\ b)$ of CWT algorithm can be calculated. A more detailed description of the spectrum-based analysis algorithm can be found in Section 3 of the Supporting Information.

2.3. PMF receptor model for source apportionment

PMF, as a factor-based receptor model, decomposes an original data matrix (X) into two separated data matrices, including the source profile matrix (F) and the source contribution matrix (G), which can be expressed as (Paatero and Tapper, 1994; Paatero, 2007; Paatero et al., 2014):

$$x_{ij} = \sum_{k=1}^{p} g_{ik} f_{kj} + e_{ij} \tag{4}$$

where x_{ij} is the concentration of jth species measured in the ith sample (time), p is the number of factors, the factor profile f_{kj} is the concentration of jth species from the kth source, and the factor time series g_{ik} is the contribution of the kth source to the ith sample (time). Meanwhile, the residual matrix e_{ij} is the error of the jth species measured in the ith sample (time). In this study, the signal-to-noise ratio (S/N) is used to select the optimal input variables. A total of 22 species are selected by the PMF receptor model, including EC, OC, NO_3^-, SO_4^{2-}, NH_4^+, Cl^-, Si, K, Ca, Cr, Mn, Fe, Ni, Cu, Zn, As, Se, Cd, Sn, Sb, Ba and Pb. A more detailed description of the PMF receptor model can be found in Section 4 of the Supporting Information.

2.4. The hybrid source apportionment framework

The hybrid source apportionment framework is developed combining the spectral analyses for spectrum characteristics extraction and the PMF receptor model for source contribution assessment of $PM_{2.5}$ pollution. A graphical scheme of this hybrid source apportionment framework is shown in Fig. 1. The steps of the source apportionment process are presented as follows:

(1) Spectrum characteristics extraction.

Step1 Select the input data with high-time resolution measurements of $PM_{2.5}$ chemical components;
Step2 Perform FFT- and CWT-based spectral analyses for the spectral conversion of $PM_{2.5}$ chemical components;
Step3 Analyze the periodic and aperiodic spectrum characteristics as necessary indicators for reliable source features;

(2) Source contribution assessment.

Step4 Apply the PMF receptor model for $PM_{2.5}$ source apportionment;
Step5 Obtain the p Factors and their contribution information;
Step6 Perform the FFT- and CWT-based spectral analyses for the spectral conversion of the Factors;
Step7 Assess the resultant Factors comparing with the spectrum characteristics of the Factors and $PM_{2.5}$ mass for an optimum solution by the hybrid framework.

3. Results and discussion

3.1. Periodic characteristics of $PM_{2.5}$ pollution

The periodic spectrum characteristics of CO, SO_2, NO_2, O_3 and $PM_{2.5}$ extracted by FFT algorithm at the sampling site are illustrated in Fig. S2. It can be inferred that only NO_2 and O_3 reflect obvious periodic features, and show the diurnal periodic pattern. Generally, NO_2 is primarily emitted from motor vehicle and coal combustion activities (Yu et al., 2019). Consequently, the periodic feature of NO_2 may be affected by the periodic features of vehicle emission and coal combustion under human activity patterns. Compared with NO_2 and O_3, the periodic features of

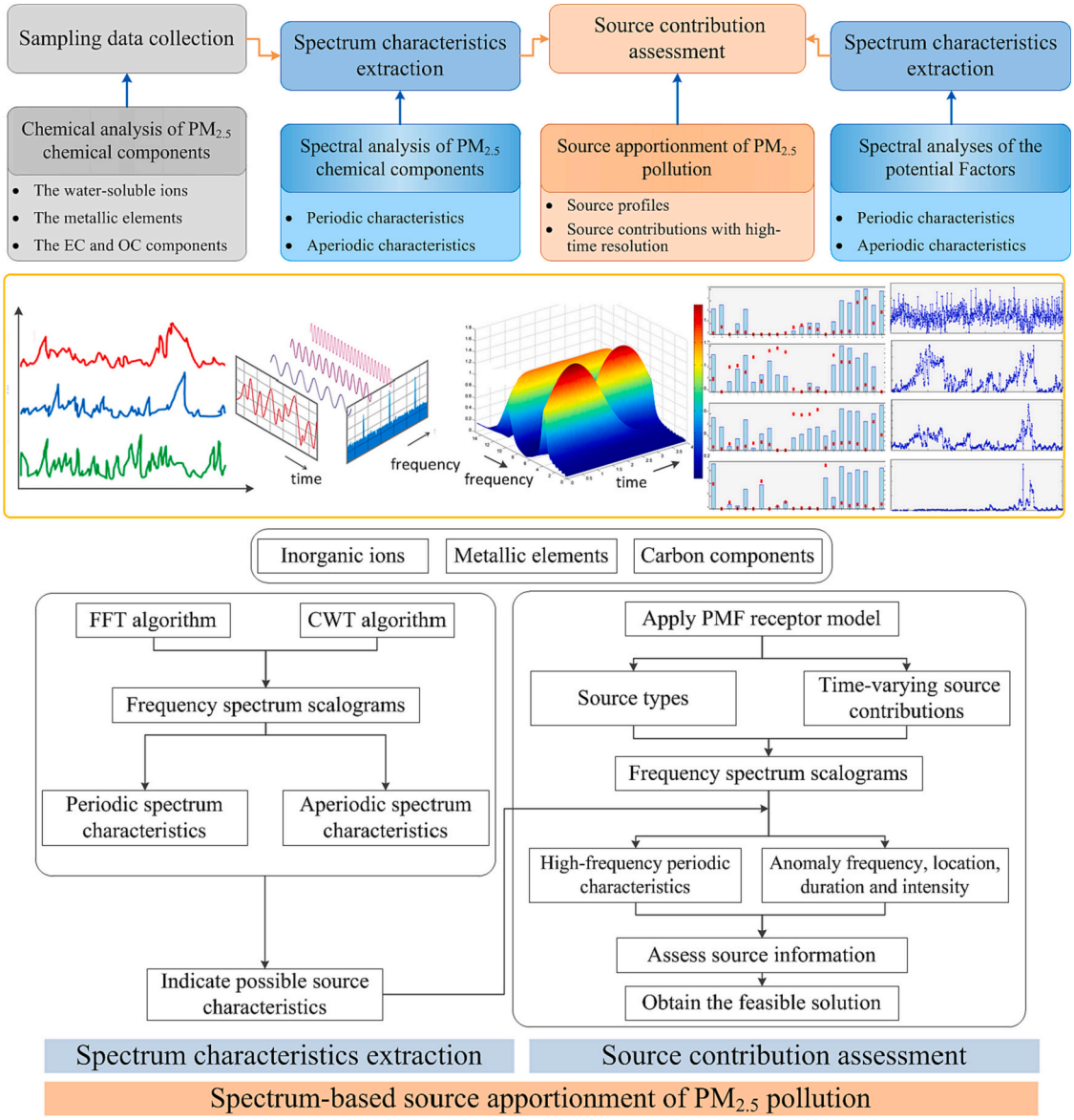

Fig. 1. Flow chart of the hybrid source apportionment framework.

CO, SO_2, and $PM_{2.5}$ cannot be observed in Fig. S2. Meanwhile, most of the concentrations of $PM_{2.5}$ chemical components present basically consistent trends with the concentrations of $PM_{2.5}$ over time. Therefore, the periodic spectrum analysis of $PM_{2.5}$ chemical components can reflect the periodic characteristics of $PM_{2.5}$ pollution and the potential interactions of pollution sources. As the typical tracers with respect to traffic-related activities (Massimi et al., 2020), the metallic elements Sb and Sn present significant periodic characteristics in Fig. S3. However, except for Sb and Sn, most of the $PM_{2.5}$ chemical components exhibit no periodic features in Fig. S4 to S6. Due to the complex meteorological conditions and diverse pollution sources, CO, SO_2, $PM_{2.5}$ and most of the $PM_{2.5}$ chemical components present aperiodic characteristics rather than periodic characteristics, which are discussed in Sections 3.2.1 and 3.2.2. A more detailed periodic spectrum result of $PM_{2.5}$ pollution can be found in Section 5 of the Supporting Information.

3.2. *Aperiodic characteristics of $PM_{2.5}$ pollution*

3.2.1. *Anomaly features of $PM_{2.5}$ and other gaseous pollutants*

The energy density distributions of CO, SO_2, NO_2, O_3 and $PM_{2.5}$ with the scaling factors ranging from 1 to 256 extracted by CWT algorithm illustrate their high-frequency anomaly features in Fig. S7. In terms of $PM_{2.5}$ mass, the aperiodic characteristics with localized abrupt increases of $PM_{2.5}$ concentrations can be captured during the winter heating period in Fig. S7(c). The CWT scalogram of $PM_{2.5}$ shows that the yellow patches representing high spectral energy areas appear on February 9, 2021 and disappear on February 15, 2021, indicating that a remarkable anomaly variation occurs over the duration of approximately 7 days during the Chinese Spring Festival. Notably, significant oscillations are observed on the scale of 128 to 224, indicating that the anomaly features of $PM_{2.5}$ show a relatively low frequency and strong amplitude during the Chinese Spring Festival. Moreover, the CWT scalogram of $PM_{2.5}$ shows medium spectral energy areas represented by blue patches on the scale of 32 to 48, which appear from February 9, 2021 to February 15, 2021. This demonstrates that a medium anomaly occurs at a relatively high-frequency domain with low amplitude during the Chinese Spring Festival. And the duration of the medium anomaly is much shorter than the duration of the strong one.

3.2.2. *Anomaly features of $PM_{2.5}$ chemical components*

The energy density distributions of $PM_{2.5}$ chemical components with the scaling factors ranging from 1 to 256 extracted by CWT algorithm

illustrate their related high-frequency anomaly features in Fig. S8 to Fig. S12. The metallic elements As, Pb, Zn and Se present similar anomaly features as $PM_{2.5}$ and CO (Fig. S8). The CWT scalograms of As, Pb, Zn and Se show that the yellow patches representing high spectral energy areas appear from January 20, 2021 to January 25, 2021 and February 9, 2021 to February 15, 2021. The energy peak appears approximately on the scale of 128 to 256, indicating that the anomalies of these elements tend to occur at a relatively low-frequency domain, which is mainly related to coal combustions. The anomaly features of the metallic elements Cd, Sb and Sn (Fig. S9) are consistent with the spectrum characteristic of NO_3^- (Fig. S12). The amplitude of the anomalies is much stronger than the one of NO_3^-. The energy peak appears

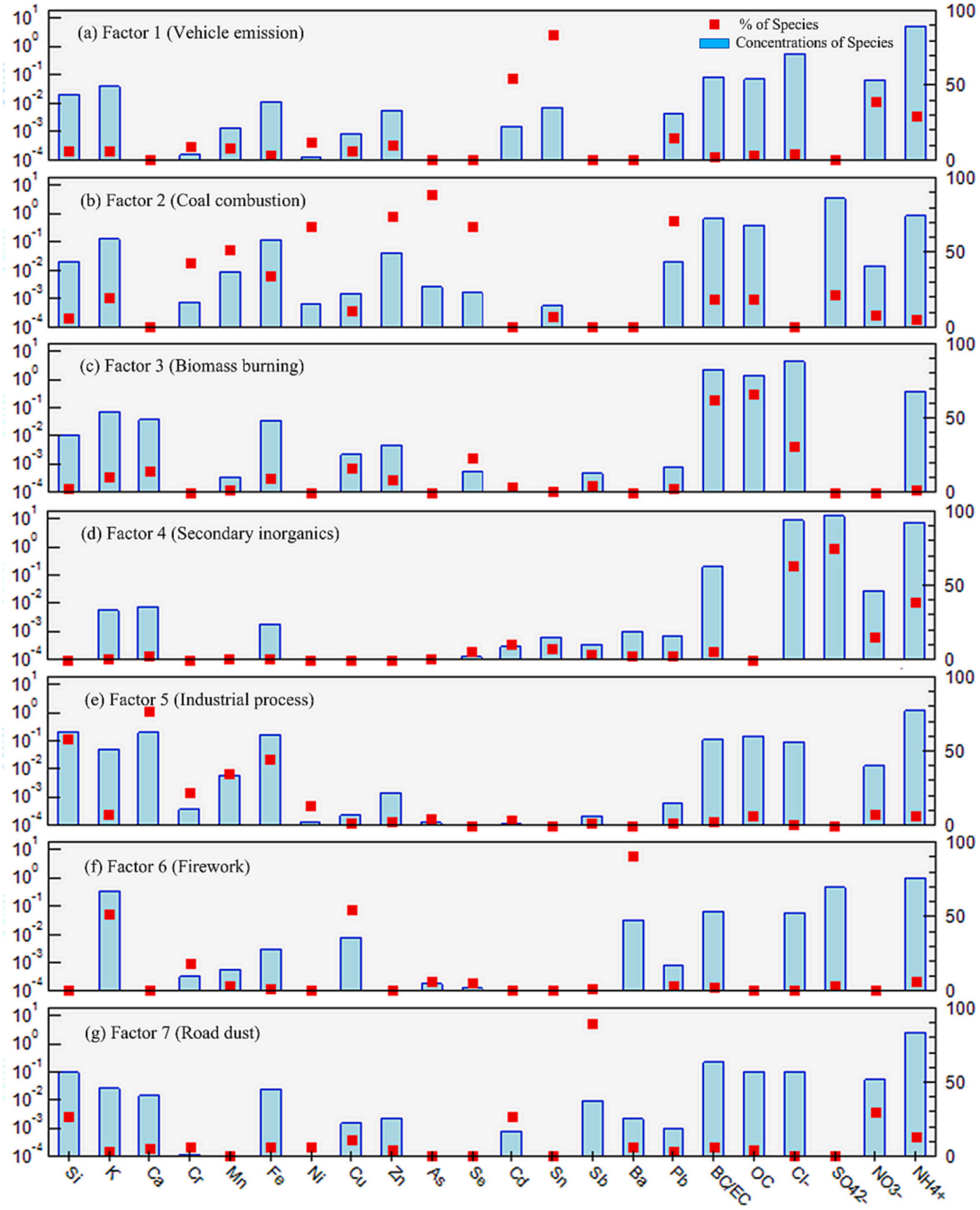

Fig. 2. The source profiles and contributions of the seven Factors by the PMF receptor model. The left y-axis represents the concentration of each species as a pale blue bar and the right y-axis represents the percentage of each species as a red box.

approximately on the scale of 16 to 64, demonstrating that the anomalies of these metallic elements tend to occur at a relatively high-frequency domain, which is generally related to vehicle emissions. As illustrated in Fig. S10, the metallic elements Ba, Cr, Cu and K demonstrate a sudden increase in a short time period. The spectral energies of these metallic elements exhibit corresponding surge shape distributions during the Chinese Spring Festival in the CWT scalogram. Actually, the metallic elements Ba, Cr, Cu and K can be emitted from the firework. Ni also shows a surge shape distribution on February 4, 2021, which can be associated with industrial activities in Fig. S10(e). The spectral energies of metallic elements Ca, Fe, Mn and Si present a similar anomaly feature of surge shape with a lower energy peak than the one of Ni (Fig. S11). The spectrum characteristics of carbon components (EC and OC) and inorganic ions (SO_4^{2-}, NH_4^+, and Cl^-) are consistent with the one of $PM_{2.5}$ (Fig. S12), and they are generally influenced by the diverse pollution sources. In summary, the spectrum characteristics extraction can reveal more intrinsic details of $PM_{2.5}$ pollutant evolution in the frequency domain, which cannot be easily observed in the time domain, to build a more sophisticated source apportionment framework. A more detailed aperiodic spectrum result of $PM_{2.5}$ pollution can be found in Section 6 of the Supporting Information.

3.3. Source apportionment of $PM_{2.5}$ pollution

In this study, spectrum-based source apportionment of $PM_{2.5}$ pollution with high-time resolution is identified in Beijing during the winter heating period. The source apportionment solution performed by the PMF receptor model is shown in Fig. 2 and Fig. S13. Seven Factors are obtained as the optimal solution assisted by the spectrum-based characteristics, including vehicle emission, coal combustion, biomass burning, secondary inorganic aerosols, industrial process, firework emission and road dust.

3.3.1. Source apportionment solution

Factor 1 is closely relevant to an indicator of vehicle emission, identified by relatively moderate proportions of metallic elements Cd, Pb, Ni, Zn, Cr and Mn from mechanical abrasion of vehicle components related to brake, tyre and clutch in Fig. 2(a) (Piscitello et al., 2021; Rai et al., 2021). The contribution from metallic element Sn (83.70 %), as one of the typical tracers with respect to rail transport, makes significant sense to Factor 1 (Almeida et al., 2020; Massimi et al., 2020). Factor 1 is also characterized by moderate contribution of NO_3^- (38.84 %), which is generally associated with traffic-related activities. The percentage of vehicle emission contributing to $PM_{2.5}$ pollution accounts for 11.00 %, which is similar to the previous studies (11.30 %-14.90 %) (Yang et al., 2016; Park et al., 2022; Zhang et al., 2023c). Factor 2 presents high proportions of As (89.27 %), Zn (74.86 %), Pb (71.82 %), Ni (67.56 %) and Se (67.32 %), and together with moderate proportions of Mn (51.75 %) and Cr (43.62 %), which is associated with a typical indicator of coal combustion (Yu et al., 2019; Rai et al., 2021). As shown in Fig. 2(b), the relatively reasonable contributions of EC, OC, and SO_4^{2-} from coal combustion are observed in this factor, accounting for 19.06 %, 18.72 %, and 22.13 %. Owing to the "coal-to-gas" transition policy in Beijing (Zhang et al., 2023b), the contribution of coal combustion accounts for approximately 10.70 % to $PM_{2.5}$ pollution during the winter heating period, which can be attributed to the related residential consumption in the rural areas upwind of Beijing (Park et al., 2022). The contribution fraction of coal combustion is in good agreement with previous researches (6.42 %-13.26 %) (Huang et al., 2017; Li et al., 2017; Lv et al., 2021; Lv et al., 2022; Park et al., 2022; Zhang et al., 2023c). Factor 3 is supposed as an indicator of biomass burning, characterized by relatively moderate contributions of the metallic element K (19.83 %) and the inorganic ion Cl^- (31.24 %) in Fig. 2(c). Since K can be emitted from wood lignin combustion, it is generally used as a primary tracer to indicate biomass burning, originating from residential biofuel, municipal solid waste and agricultural waste (Smith et al., 2017; Rai et al., 2021). Besides, OC (66.31 %) also provides substantial contribution to this factor. Factor 3 makes a relatively significant contribution accounting for 15.01 % to $PM_{2.5}$ pollution, which may be due to the intensive biomass burning for cooking and heating activities by residents in Beijing during the winter heating period. The contribution of biomass burning in this study is similar to the earlier studies (11.20 %-18.4 %) (Yang et al., 2016; Lv et al., 2022; Zhang et al., 2023c).

Secondary inorganic aerosols are typically characterized by significant contributions from NO_3^-, SO_4^{2-}, and NH_4^+, which is consistent with the result of Factor 4 in Fig. 2(d). Noteworthy, the proportions of the contributions of SO_4^{2-}, NH_4^+ and NO_3^- account for 75.08 %, 39.11 % and 15.69 %, respectively. As one of the dominant pollution sources, the contribution of secondary inorganic aerosols to $PM_{2.5}$ pollution is up to 50.59 %, indicating that secondary inorganic aerosols have a crucial impact on the haze episodes in Beijing during the winter heating period. The percentage of this source contributing to $PM_{2.5}$ pollution is within a similar range to the previous studies (40.50 %-52.00 %) (Huang et al., 2017; Li et al., 2017; Liu et al., 2019; Lv et al., 2022; Park et al., 2022; Zhang et al., 2023c). Factor 5 is characterized by relatively significant proportions of metallic elements Ca, Fe, Si, Mn and Cr, which are mainly emitted from industrial production, such as iron/steel and other metal manufacturing (Tian et al., 2018; Massimi et al., 2020). Hence, Factor 5 is identified as an indicator of industrial process. Due to heavily scaled-back industrial production in Beijing, the percentage of industrial process contributing to $PM_{2.5}$ pollution only accounts for 3.88 % and may be caused by the industrial-related activities in adjacent provinces. The contribution of industrial process is consistent with the earlier studies (3.20 %-6.81 %) (Huang et al., 2017; Lv et al., 2022; Zhang et al., 2023c). Factor 6 is supposed as an indicator of firework emission. Since high Ba, K and Cu are generally emitted from fireworks (Yu et al., 2019; Manchanda et al., 2022), the markedly high contributions of Ba, Cu, K and Cr to this Factor, accounting for 91.17 %, 54.79 %, 51.72 %, and 18.32 % in Fig. 2(f), are attributed to firework emission which may come from the surrounding areas of Beijing during the Chinese Spring Festival. This Factor makes a slight contribution accounting for 3.51 % to $PM_{2.5}$ pollution, which is similar to the previous studies (1.90 %-4.00 %) (Zhang et al., 2023b; Zhang et al., 2023c). Factor 7 is identified as road dust by a mainly impact from deposited anthropogenic emissions, such as road surface abrasion with dominant metallic element Sb (89.53 %) and road dust re-suspension with typical tracers Si (26.55 %), Fe (6.43 %) and Ca (6.25 %) in Fig. 2(g), which primarily refers to traffic-related dust emissions during the study period in Beijing. The contribution of road dust to $PM_{2.5}$ pollution accounts for 5.31 %, which is similar to the earlier studies (1.81 %-6.82 %) (Li et al., 2017; Liu et al., 2019; Lv et al., 2021; Lv et al., 2022; Park et al., 2022; Zhang et al., 2023c). Noteworthy, this solution with seven-Factor sources is highly consistent with the studies by Lv et al. (2022) and Zhang et al. (2023c) conducted at the heating winter period in Beijing shown in Table S1. A more detailed source apportionment result of $PM_{2.5}$ pollution and comparison among various studies can be found in Section 7 and Section 8 of the Supporting Information.

3.3.2. Driving factor analysis of the source profiles

The correlation analysis results between pollution sources and meteorological parameters are shown in Fig. 3. It can be observed that there is no obvious correlation between Factor 1 and meteorological parameters, suggesting that Factor 1 tends to be influenced primarily by human activities. The situation is the same with Factor 7. Factors 2, 3 and 4 illustrate obvious temporal variations with remarkably high contributions during the extremely cold period from January 20 to January 25 (Episode 1) and the Chinese Spring Festival from February 9 to February 15 (Episode 2) as shown in Fig. S13. In Fig. 3, the relatively strong correlation coefficients with relative humidity are 0.62, 0.53 and 0.54, respectively, implying that Factors 2, 3, and 4 are influenced not only by human activities, but also by meteorological conditions to some extent. Since industrial processes are generally not affected by the

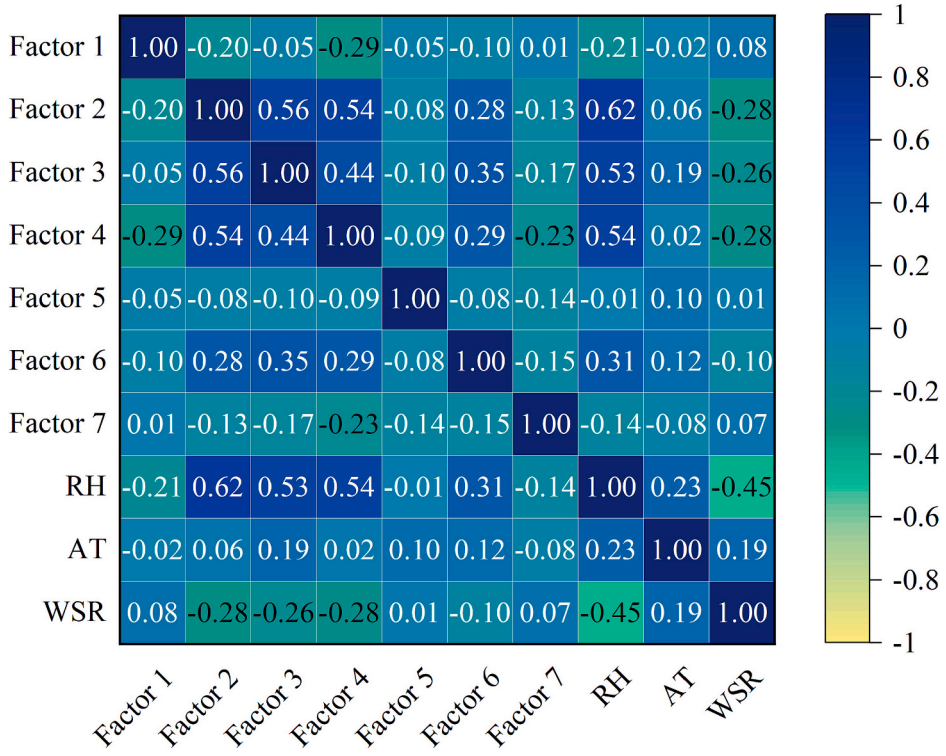

Fig. 3. The correlation analysis results of the seven Factors in relation to meteorological parameters.

meteorological conditions in Fig. 3, a relatively low and steady contribution of Factor 5 can be observed as shown in Fig. S13(e). There is a sharp increase of normalized contributions in Fig. S13(f), and this sharp peak in a short time period is associated with massive firework-related activities in the surrounding areas in Beijing during Episode 2. In addition, a moderate correlation relationship ($r = 0.31$) can be found between Factor 6 and relative humidity (Fig. 3), which suggests that the contribution of firework emission to $PM_{2.5}$ pollution is mainly resulted from human activities. In fact, air temperature also plays a vital role in the contributions of some sources discussed above to $PM_{2.5}$ pollution. The low correlation relationship may be attributed to the fact that this study only concentrates on the winter heating period rather than the entire year. A more detailed correlation analysis result can be found in Section 9 of the Supporting Information.

3.3.3. *Spectrum characteristics analysis of the source profiles*

Besides the contributions of these seven Factors discussed above, the spectrum characteristics can be used as reliable explanations for $PM_{2.5}$ source apportionment solution. The potential pollution sources identified in the seven Factors as the optimal PMF solution are in agreement with the spectrum characteristics of the seven Factors.

(1) Periodic spectrum characteristics.

The periodic spectrum characteristics of the seven Factors extracted by FFT algorithm are shown in Fig. S15. Factors 1 and 7 exhibit obvious periodic features at different frequencies, such as diurnal, semi-diurnal, eight-hourly or six-hourly periods due to the influences of natural environment cycle and human activity patterns. Generally, traffic-related activities are supposed to show diurnal or semi-diurnal patterns with relatively low contributions during the afternoon and high contributions during rush hours. These high-frequency characteristics of vehicle emission and road dust are approximately consistent with the time-varying variation tendencies of traffic-related activities, which can be used to assist PMF receptor model distinguish vehicle emission and road dust sources from other pollution sources.

(2) Aperiodic spectrum characteristics.

The energy density distributions of the seven Factors with the scaling factors ranging from 1 to 256 extracted by CWT algorithm are shown in Fig. 4. Factors 1 and 7 present unique temporal variations with continuous zigzag variation features compared with other Factors. The spectrum characteristics of Factors 1 and 7 is correspondent to the ones of Cd, Sb, Sn and NO_3^- (Fig. S9 and S12(f)), indicating that these elements act as the primary drivers to the traffic-related activities, such as vehicle emission and road dust, which are consistent with PMF source apportionment solution. The spectrum characteristic of Factor 2 shows high similarity to the ones of As, Pb, Zn, Se and SO_4^{2-} (Fig. S8 and S12 (d)) which are mainly emitted from coal combustion. And its spectral energy distribution in a relatively low-frequency domain (the scale of 192 to 224) shows that the contribution exists throughout the entire heating period, especially in the cold period (Episode 1). The spectrum characteristic of Factor 3 show high similarities to the ones of EC, OC, Cl^- and NH_4^+, which are associated with biomass burning (Fig. S12). Factor 3 is characterized by high spectral energy distribution in a relatively low-frequency domain (the scale of 128 to 160), revealing that the contribution mainly exists in the Chinese Spring Festival (Episode 2). Factor 4 is influenced by synergistic effect between Factors 2 and 3, showing high spectral energy distributions both on the scales of 128 to 160 and 192 to 224, especially in the Episode 2. Although Factors 2, 3 and 4 show a high consistency in time domain, the unique spectrum characteristic of Factor 4 can assist PMF receptor model to make secondary inorganic aerosols distinguished from biomass burning and coal combustion sources. Meanwhile, the spectrum characteristics of Factors 2, 3 and 4 are also highly consistent with the one of $PM_{2.5}$, which further explains that coal combustion, biomass burning and secondary inorganic sources have great impacts on the temporal evolution of $PM_{2.5}$ pollution during the winter heating period in Beijing. This phenomenon also assists PMF receptor model to make these three typical pollution sources distinguishable from other pollution sources. Fig. 4(e) illustrates that the spectrum characteristic of Factor 5 is related to the ones of Ca, Fe, Mn and Ni (Fig. S10(e) and S11), which are the major products from

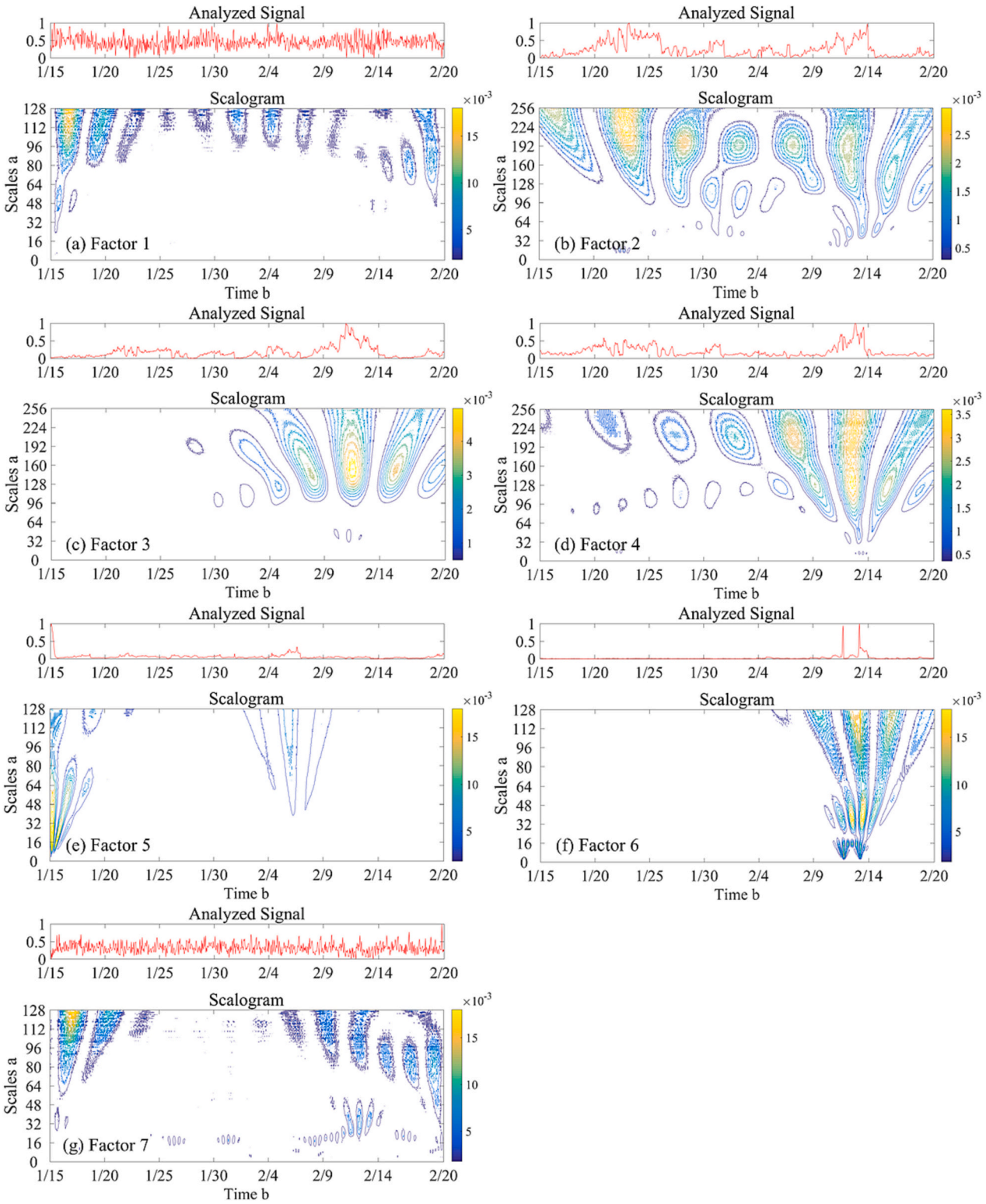

Fig. 4. The aperiodic spectrum characteristics of the seven Factors (a) Factor 1, (b) Factor 2, (c) Factor 3, (d) Factor 4, (e) Factor 5, (f) Factor 6 and (g) Factor 7 by CWT algorithm. The contour lines represent energy density distribution corresponding to the anomaly intensity indicated by the scale bar on the right, with the yellow parts representing strong anomalies, and the blue parts representing weak anomalies.

industrial process. The spectrum characteristic of Factor 6 mainly shows high spectral energy distribution in a relatively high-frequency domain (the scale of 32 to 48) in Fig. 4(f), which is similar to the ones of Ba, Cu and K (Fig. S10). These elements are typically linked with firework emissions. Although the metallic elements Cu and Ba are also enriched in traffic emissions, Factor 6 can be distinguished from Factor 1 according to the periodic and aperiodic spectrum characteristics based on the FFT- and CWT-based spectral analyses.

Spectral analyses for periodic and aperiodic characteristics can provide specific evidences to assist PMF receptor model to distinguish among diverse pollution sources. The comparisons between the spectrum characteristics of the related chemical components and the ones of

seven Factors can provide substantial supports for spectrum-based source apportionment of $PM_{2.5}$ pollution, indicating that the PMF solution is reasonable and time-varying contributions are in accordance with the factual conditions in both frequency and time domains. Moreover, the energy density distribution of $PM_{2.5}$ with the scaling factors ranging from 1 to 512 extracted by CWT algorithm illustrates the relatively low-frequency anomaly features in Fig. S16(a). Besides the high-frequency anomaly features on the scales of 32 to 48, 128 to 160 and 192 to 224 in Fig. S7(c), low-frequency anomaly features can also be observed on the scale of 320 to 448 of $PM_{2.5}$. The driving factors of $PM_{2.5}$ pollution are related to natural conditions and human activities. Generally, meteorological conditions are impacted by the solar radiation following seasonal, half-yearly and yearly variations, and contribute to the low-frequency anomaly features of $PM_{2.5}$ pollution (Kirchner, 2016). And human activities are likely to lead to high-frequency transient anomalies from point source inputs, mobile source inputs and surface source inputs (Jiang et al., 2020). According to Fig. S16(b), the low-frequency anomaly features of $PM_{2.5}$ tend to be influenced by relative humidity to some extent. And the high-frequency anomaly features of $PM_{2.5}$ may result from at least three source inputs with different high-frequency patterns. The aperiodic spectrum characteristics with four different high-frequency patterns (Factors 2, 3, 4 and 6) are in accord with the abovementioned discussions according to the seven-Factor source apportionment solution in Fig. 4. Since PMF receptor model requires a detailed analysis for the chemical compositions of the potential sources and a reconstructed pollution source are inevitably influenced by other potential pollution sources, it sometimes cannot provide a reasonable description for all the source profiles, even cannot separate or distinguish the sources absolutely with a similar chemical composition due to the absence of key species (Schleicher and Weiss, 2023). In this study, spectrum-based source apportionment of $PM_{2.5}$ pollution without source profiles of EC and OC is identified in Beijing during the same sampling period. The source apportionment solution and spectrum characteristics of the seven Factors are shown in Fig. S17 and S18. Since the metallic elements Si, Ca, Fe, Cu and Mn, as the reliable tracers, are enriched in multiple pollution sources, it is hard to distinguish among coal combustion, industrial process and road dust without EC and OC to some extent in this study. However, the FFT- and CWT-based spectral analyses can provide the related quantitative frequency-based descriptions and explanations to assist PMF receptor model to obtain the optimal source apportionment solution. A more detailed spectrum characteristics analysis of the source profiles can be found in Section 10 of the Supporting Information.

4. Conclusions

In this study, a spectrum-based source apportionment framework is developed combining the FFT- and CWT-based spectral analyses for source spectrum characteristics extraction and the PMF receptor model for source contribution assessment of $PM_{2.5}$ pollution. The spectrum-based source apportionment framework is applied to Beijing during the winter heating period with 1-h time resolution. According to the spectral analyses, Factors 1 and 7 exhibit obvious periodic features at different frequencies, such as diurnal, semi-diurnal, eight-hourly or six-hourly periods, which are approximately consistent with the traffic-related activities. Although Factors 2, 3 and 4 show a high consistency in time domain, Factor 4 is influenced by synergistic effect between Factors 2 and 3, which show relatively low-frequency anomaly features on the scales of 128 to 160 and 192 to 224, respectively. The spectrum characteristic of Factor 6 reflects a relatively high-frequency anomaly feature on the scale of 32 to 48. The spectrum characteristics extraction can reveal more intrinsic details of $PM_{2.5}$ pollutant evolution in the frequency domain, which cannot be easily observed in the time domain, to assist PMF receptor model to distinguish among diverse pollution sources. Finally, seven major pollution sources, i.e. secondary inorganic aerosols (50.59 %), biomass burning (15.01 %), vehicle emission (11.00 %), coal combustion (10.70 %), road dust (5.31 %), industrial process (3.88 %) and firework emission (3.51 %) are identified to make relatively significant contributions to $PM_{2.5}$ pollution in Beijing during the winter heating period.

The results reflect that (a) the developed framework can capture more details of $PM_{2.5}$ pollutant evolution both on the frequency and time domains to provide sophisticated indicators for source apportionment; (b) the developed framework can gain a specific understanding of the source information to select the optimal source apportionment solution assisted by the spectrum characteristics of $PM_{2.5}$ and related chemical components; (c) the developed framework can distinguish the contributions of various pollution sources and provide reasonable explanations based on the spectrum characteristics of multiple Factors. The developed source apportionment framework could be a promising pathway to harmonize the spectral analysis and receptor model for spectrum-based source apportionment of $PM_{2.5}$ pollution. In the future, parameter optimization algorithm is planned to be added into PMF receptor model to optimize the proportions of the profiles in each Factor for a more satisfactory and reasonable PMF result. Meanwhile, rule-based inference algorithm is also considered to automatically judge potential source information according to the proportions of the profiles, correlation analysis and frequency spectrum characteristics for an intelligent source apportionment.

CRediT authorship contribution statement

Jie Liu: Conceptualization, Methodology, Writing – original draft, Writing – review & editing. **Fangjingxin Ma:** Data curation, Methodology, Software, Formal analysis. **Tse-Lun Chen:** Formal analysis, Resources, Writing – review & editing. **Dexun Jiang:** Software, Investigation, Resources. **Meng Du:** Methodology, Investigation. **Xiaole Zhang:** Data curation, Validation. **Xiaoxiao Feng:** Investigation, Data curation. **Qiyuan Wang:** Data curation, Validation, Resources. **Junji Cao:** Data curation, Visualization. **Jing Wang:** Conceptualization, Formal analysis, Supervision, Visualization.

Declaration of competing interest

The authors declare that they have no known competing financial interests or personal relationships that could have appeared to influence the work reported in this paper.

Data availability

Data will be made available on request.

Acknowledgements

This research was supported by the National Natural Science Foundation of China (Grant No.52000022), China Postdoctoral Science Foundation (Grant No. 2022T150105), Natural Science Foundation of Heilongjiang Province (Grant No.YQ2021E004), Heilongjiang Postdoctoral Scientific Research Development Fund (Grant No. LBH-Q20068), and the project Clean Air China sponsored by Swiss Agency for Development and Cooperation (Grant No. 7F-09802.01.03). Liu, J. and Jiang, D.X. are extremely grateful to the financial support from the China Scholarship Council (CSC).

Appendix A. Supplementary data

Supplementary data to this article can be found online at https://doi.org/10.1016/j.scitotenv.2023.169055.

References

Alias, N.F., Khan, M.F., Sairi, N.A., Zain, S.M., Suradi, H., Rahim, A., Banerjee, T., Bari, M.A., Othman, M., Latif, M.T., 2020. Characteristics, emission sources, and risk factors of heavy metals in $PM_{2.5}$ from Southern Malaysia. ACS Earth Space Chem. 4, 1309–1323.

Almeida, S.M., Manousakas, M., Diapouli, E., Kertesz, Z., Samek, L., Hristova, E., Šega, K., Alvarez, R.P., Belis, C.A., Eleftheriadis, K., 2020. Ambient particulate matter source apportionment using receptor modelling in European and Central Asia urban areas. Environ. Pollut. 266 (Part 3), 115199.

Balachandran, S., Chang, H.H., Pachon, J.E., Holmes, H.A., Mulholland, J.A., Russell, A. G., 2013. Bayesian-based ensemble source apportionment of $PM_{2.5}$. Environ. Sci. Technol. 47, 13511–13518.

Barmpadimos, I., Nufer, M., Oderbolz, D.C., Keller, J., Aksoyoglu, S., Hueglin, C., Baltensperger, U., Prévôt, A.S., 2011. The weekly cycle of ambient concentrations and traffic emissions of coarse (PM_{10}–$PM_{2.5}$) atmospheric particles. Atmos. Environ. 45 (27), 4580–4590.

Bland, G.D., Battifarano, M., Liu, Q., Yang, X.Z., Lu, D.W., Jiang, G.B., Loery, G.V., 2022. Single-particle metal fingerprint analysis and machine learning pipeline for source apportionment of metal-containing fine particles in air. Environ. Sci. Technol. Lett. https://doi.org/10.1021/acs.estlett.2c00835.

Chang, P.K., Griffith, S.M., Chuang, H.C., Chuang, K.J., Wang, Y.H., Chang, K.E., Hsiao, T.C., 2022. Particulate matter in a motorcycle-dominated urban area: source apportionment and cancer risk of lung deposited surface area (LDSA) concentrations. J. Hazard. Mater. 427, 128188.

Chen, X.B., Yin, L.R., Fan, Y.L., Song, L.H., Ji, T.T., Liu, Y., Tian, J.W., Zheng, W.F., 2020. Temporal evolution characteristics of $PM_{2.5}$ concentration based on continuous wavelet transform. Sci. Total Environ. 699, 134244.

Chen, K., Xu, J.S., Famiyeh, L., Sun, Y., Ji, D.S., Xu, H.H., Wang, C.J., Metcalfe, S.E., Betha, R., Behera, S.N., Jia, C.R., Xiao, H., He, J., 2022. Chemical constituents, driving factors, and source apportionment of oxidative potential of ambient fine particulate matter in a Port City in East China. J. Hazard. Mater. 440, 129864.

Chen, T.L., Lai, C.H., Chen, Y.C., Ho, Y.H., Chen, A.Y., Hsiao, T.C., 2023. Source-oriented risk and lung-deposited surface area (LDSA) of ultrafine particles in a Southeast Asia urban area. Sci. Total Environ. 870, 161733.

Chi, W.J., Lin, Y.C., 2021. Investigation of the main $PM_{2.5}$ sources and diffusion patterns and corresponding meteorological conditions by the wavelet analysis approach. Atmos. Pollut. Res. 12, 101222.

Cooley, J.W., Tukey, J.W., 1965. An algorithm for the machine calculation of complex Fourier series. Math. Comput. 19 (90), 297–301.

Crilley, L.R., Lucarelli, F., Bloss, W.J., Harrison, R.M., Beddows, D.C., Calzolai, G., Nava, S., Valli, G., Bernardoni, V., Vecchi, R., 2017. Source apportionment of fine and coarse particles at a roadside and urban background site in London during the 2012 summer ClearfLo campaign. Environ. Pollut. 220, 766–778.

Feng, J.L., Yu, H., Su, X.F., Liu, S.H., Li, Y., Pan, Y.P., Sun, J.H., 2016. Chemical composition and source apportionment of $PM_{2.5}$ during Chinese spring festival at Xinxiang, a heavily polluted city in North China: fireworks and health risks. Atmos. Res. 182, 176–188.

Hsiao, T.C., Chou, L.T., Pan, S.Y., Young, L.H., Chi, K.H., Chen, A.Y., 2021. Chemically and temporally resolved oxidative potential of urban fine particulate matter. Environ. Pollut. 291, 118206.

Huang, X.J., Liu, Z.R., Liu, J.Y., Hu, B., Wen, T.X., Tang, G.Q., Zhang, J.K., Wu, F.K., Ji, D.S., Wang, L.L., Wang, Y.S., 2017. Chemical characterization and source identification of $PM_{2.5}$ at multiple sites in the Beijing-Tianjin-Hebei region, China. Atmos. Chem. Phys. 17, 12941–12962.

Jiang, J.P., Zheng, Y., Pang, T.R., Wang, B.Y., Chachan, R., Tian, Y., 2020. A comprehensive study on spectral analysis and anomaly detection of river water quality dynamics with high time resolution measurements. J. Hydrol. 589, 125175.

Kim, S., Kim, T.Y., Yi, S.M., Heo, J., 2018. Source apportionment of $PM_{2.5}$ using positive matrix factorization (PMF) at a rural site in Korea. J. Environ. Manag. 214, 325–334.

Kirchner, J.W., 2016. Aggregation in environmental systems - part 1: seasonal tracer cycles quantify young water fractions, but not mean transit times, in spatially heterogeneous catchments. Hydrol. Earth Syst. Sci. 20 (1), 279–297.

Lei, Y.L., Shen, Z.X., Zhang, T., Lu, D., Zeng, Y.L., Zhang, Q., Xu, H.M., Bei, N.F., Wang, X., Cao, J.J., 2019. High time resolution observation of $PM_{2.5}$ Brown carbon over Xi'an in northwestern China: seasonal variation and source apportionment. Chemosphere 237, 124530.

Li, P., Kong, F., He, Q., Liu, Y., 2013. Multiscale slope feature extraction for rotating machinery fault diagnosis using wavelet analysis. Measurement 46, 497–505.

Li, Y.Y., Chang, M.A., Ding, S.S., Wang, S.W., Ni, D., Hu, H.T., 2017. Monitoring and source apportionment of trace elements in $PM_{2.5}$: implications for local air quality management. J. Environ. Manag. 196, 16–25.

Li, S., Liu, N.J., Tang, L.F., Zhang, F.T., Liu, J.H., Liu, J.K., 2021. Mutation test and multiple-wavelet coherence of $PM_{2.5}$ concentration in Guiyang, China. Air Qual. Atmos. Health 14 (7), 955–966.

Liu, Y., Zheng, M., Yu, M.Y., Cai, X.H., Du, H.Y., Li, J., Zhou, T., Yan, C.Q., Wang, X.S., Shi, Z.B., Harrison, R.M., Zhang, Q., He, K., 2019. High-time-resolution source apportionment of $PM_{2.5}$ in Beijing with multiple models. Atmos. Chem. Phys. 19 (9), 6595–6609.

Liu, X., Zhang, X., Schnelle-Kreis, J., Jakobi, G., Cao, X., Cyrys, J., Yang, L., Schloter-Hai, B., Abbaszade, G., Orasche, J., Khedr, M., Kowalski, M., Hank, M., Zimmermann, R., 2020. Spatiotemporal characteristics and driving factors of black carbon in Augsburg, Germany: combination of mobile monitoring and street view images. Environ. Sci. Technol. 55 (1), 160–168.

Lv, L.L., Chen, Y.J., Han, Y., Cui, M., Wei, P., Zheng, M., Hu, J.N., 2021. High-time-resolution $PM_{2.5}$ source apportionment based on multi-model with organic tracers in Beijing during haze episodes. Sci. Total Environ. 772, 144766.

Lv, L.L., Wei, P., Hu, J.N., Chen, Y.J., Shi, Y.P., 2022. Source apportionment and regional transport of $PM_{2.5}$ during haze episodes in Beijing combined with multiple models. Atmos. Res. 266, 105957.

Ma, W., Ding, J.L., Wang, R., Wang, J.L., 2022. Drivers of $PM_{2.5}$ in the urban agglomeration on the northern slope of the Tianshan Mountains, China. Environ. Pollut. 309, 119777.

Manchanda, C., Kumar, M., Singh, V., Hazarika, N., Faisal, M., Lalchandani, V., Shukla, A., Dave, J., Rastogi, N., Tripathi, S.N., 2022. Chemical speciation and source apportionment of ambient $PM_{2.5}$ in New Delhi before, during, and after the Diwali fireworks. Atmos. Pollut. Res. 13, 101428.

Manousakas, M., Furger, M., Daellenbach, K.R., Canonaco, F., Chen, G., Tobler, A., Rai, P., Qi, L., Tremper, A.H., Green, D., Hueglin, C., Slowik, J.G., Haddad, I.E., Prevot, A.S.H., 2022. Source identification of the elemental fraction of particulate matter using size segregated, highly time-resolved data and an optimized source apportionment approach. Atmos. Environ. X 14, 100165.

Masiol, M., Hopke, P.K., Felton, H.D., Frank, B.P., Rattigan, O.V., Wurth, M.J., LaDuke, G.H., 2017. Source apportionment of $PM_{2.5}$ chemically speciated mass and particle number concentrations in new York City. Atmos. Environ. 148, 215–229.

Massimi, L., Ristorini, M., Astolfi, M.L., Perrino, C., Canepari, S., 2020. High resolution spatial mapping of element concentrations in PM_{10}: a powerful tool for localization of emission sources. Atmos. Res. 244, 105060.

Munoz, A., Ertlé, R., Unser, M., 2002. Continuous wavelet transform with arbitrary scales and O (N) complexity. Signal Process. 82 (5), 749–757.

Olson, M.R., Victoria Garcia, M., Robinson, M.A., Van Rooy, P., Dietenberger, M.A., Bergin, M., Schauer, J.J., 2015. Investigation of black and brown carbon multiple wavelength-dependent light absorption from biomass and fossil fuel combustion source emissions. J. Geophys. Res. Atmos. 120 (13), 6682–6697.

Paatero, P., 2007. User's Guide for Positive Matrix Factorization Programs PMF2 and PMF3, Part 1–2: Tutorial, 19–21. University of Helsinki, Helsinki, Finland.

Paatero, P., Tapper, U., 1994. Positive matrix factorization: a non-negative factor model with optimal utilization of error estimates of data values. Environmetrics 5, 111–126.

Paatero, P., Eberly, S., Brown, S.G., Norris, G.A., 2014. Methods for estimating uncertainty in factor analytic solutions. Atmos. Meas. Tech. 7 (3), 781–797.

Park, M.B., Lee, T.J., Lee, E.S., Kim, D.S., 2019. Enhancing source identification of hourly $PM_{2.5}$ data in Seoul based on a dataset segmentation scheme by positive matrix factorization (PMF). Atmos. Pollut. Res. 10, 1042–1059.

Park, J., Kim, H., Kim, Y., Heo, J., Kim, S.W., Jeon, K., Yi, S.M., Hopke, P.K., 2022. Source apportionment of $PM_{2.5}$ in Seoul, South Korea and Beijing, China using dispersion normalized PMF. Sci. Total Environ. 833, 155056.

Piscitello, A., Bianco, C., Casasso, A., Sethi, R., 2021. Non-exhaust traffic emissions: sources, characterization, and mitigation measures. Sci. Total Environ. 766, 144440.

Rai, V.K., Mohanty, A.R., 2007. Bearing fault diagnosis using FFT of intrinsic mode functions in Hilbert–Huang transform. Mech. Syst. Signal Process. 21 (6), 2607–2615.

Rai, P., Furger, M., Slowik, J.G., Zhong, H.B., Tong, Y.D., Wang, L.W., Duan, J., Gu, Y.F., Qi, L., Huang, R.J., Cao, J.J., Baltensperger, U., Prevot, A.S.H., 2021. Characteristics and sources of hourly elements in PM_{10} and $PM_{2.5}$ during wintertime in Beijing. Environ. Pollut. 278, 116865.

Rajaby, E., Sayedi, S.M., 2022. A structured review of sparse fast Fourier transform algorithms. Digit. Signal Process. 123, 103403.

Schleicher, N.J., Weiss, D.J., 2023. Identification of atmospheric particulate matter derived from coal and biomass burning and from non-exhaust traffic emissions using zinc isotope signatures. Environ. Pollut. 329, 121664.

Smith, P.C., Jeong, C.H., Healy, R.M., Zlotorzynska, D.E., Celo, V., Brook, J.R., Evans, G., 2017. Sources of particulate matter components in the Athabasca oil sands region: investigation through a comparison of trace element measurement methodologies. Atmos. Chem. Phys. 17 (15), 9435–9449.

Srivastava, D., Xu, J.S., Vu, T.V., Liu, D., Li, L.J., Fu, P.Q., Hou, S.Q., Palmerola, N.M., Shi, Z.B., Palmerola, R.M., 2021. Insight into $PM_{2.5}$ sources by applying positive matrix factorization (PMF) at urban and rural sites of Beijing. Atmos. Chem. Phys. 21, 14703–14724.

Stanek, L.W., Sacks, J.D., Dutton, S.J., Dubois, J.J.B., 2011. Attributing health effects to apportioned components and sources of particulate matter: an evaluation of collective results. Atmos. Environ. 45 (32), 5655–5663.

Taghvaee, S., Sowlat, M.H., Mousavi, A., Hassanvand, M.S., Yunesian, M., Naddafi, K., Sioutas, C., 2018. Source apportionment of ambient $PM_{2.5}$ in two locations in central Tehran using the Positive Matrix Factorization (PMF) model. Sci. Total Environ. 628–629, 672–686.

Tao, J., Zhang, L.M., Cao, J.J., Zhong, L.J., Chen, D.S., Yang, Y.H., Chen, D.H., Chen, L. G., Zhang, Z.S., Wu, Y.F., Xia, Y.J., Ye, S.Q., Zhang, R.J., 2017. Source apportionment of $PM_{2.5}$ at urban and suburban areas of the Pearl River Delta region, south China -With emphasis on ship emissions. Sci. Total Environ. 574, 1559–1570.

Tary, J.B., Herrera, R.H., van der Baan, M., 2018. Analysis of time-varying signals using continuous wavelet and synchrosqueezed transforms. Philos. Trans. R. Soc. A Math. Phys. Eng. Sci. 376 (2126), 20170254.

Tian, Y.Z., Liu, J.Y., Han, S.Q., Shi, X.R., Shi, G.L., Xu, H., Yu, .F., Zhang, Y.F., Feng, Y.C., Russell, A.G., 2018. Spatial, seasonal and diurnal patterns in physicochemical characteristics and sources of $PM_{2.5}$ in both inland and coastal regions within a megacity in China. J. Hazard. Mater., 342, 139–149.

Tobler, A., Bhattu, D., Canonaco, F., Lalchandani, V., Shukla, A., Thamban, N.M., Mishra, S., Srivastava, A.K., Bisht, D.S., Tiwari, S., Singh, S., Močnik, G., Baltensperger, U., Tripathi, S.N., Slowik, J.G., Prévôt, A.S.H., 2020. Chemical

characterization of $PM_{2.5}$ and source apportionment of organic aerosol in New Delhi, India. Sci. Total Environ. 745, 140924.
Vedantham, R., Landis, M.S., Olson, D., Pancras, J.P., 2014. Source identification of $PM_{2.5}$ in Steubenville, Ohio using a hybrid method for highly time-resolved data. Environ. Sci. Technol. 48, 1718–1726.
Veld, M., Alastuey, A., Pandolfi, M., Amato, F., Pérez, N., Reche, C., Via, M., Minguillón, M.C., Escudero, M., Querol, X., 2021. Compositional changes of $PM_{2.5}$ in NE Spain during 2009–2018: a trend analysis of the chemical composition and source apportionment. Sci. Total Environ. 795, 148728.
Yang, H.N., Chen, J., Wen, J.J., Tian, H.Z., Liu, X.G., 2016. Composition and sources of $PM_{2.5}$ around the winter heating period of 2013 and 2014 in Beijing: implications for efficient mitigation measures. Atmos. Environ. 124, 378–386.
Yu, Y.Y., He, S.Y., Wu, X.L., Zhang, C., Yao, Y., Liao, H., Wang, Q.G., Xie, M.J., 2019. $PM_{2.5}$ elements at an urban site in Yangtze River Delta, China: high time-resolved measurement and the application in source apportionment. Environ. Pollut. 253, 1089–1099.
Yu, T.L., Wang, Y., Huang, J., Liu, X., Li, J.B., Zhan, W., 2022. Study on the regional prediction model of $PM_{2.5}$ concentrations based on multi-source observations. Atmospheric. Pollut. Res. 13 (4), 101363.
Zhang, C., Zhang, Y.Y., Liu, X.A., Liu, Y.F., Li, C.L., 2023a. Characteristics and source apportionment of $PM_{2.5}$ under the dual influence of the spring festival and the COVID-19 pandemic in Yuncheng city. J. Environ. Sci. 125, 553–567.
Zhang, X.L., Feng, X.X., Tian, J., Zhang, Y., Li, Z.Y., Wang, Q.Y., Cui, J.J., Wang, J., 2023b. Dynamic harmonization of source-oriented and receptor models for source apportionment. Sci. Total Environ. 859, 160312.
Zhang, Y., Tian, J., Wang, Q.Y., Qi, L., Manousakas, M.I., Han, Y.M., Ran, W.K., Sun, Y.L., Liu, H.K., Zhang, R.J., Wu, Y.F., Cui, T.Q., Daellenbach, K.R., Slowik, J.G., Prévôt, A. H., Cao, J.J., 2023c. High-time-resolution chemical composition and source apportionment of $PM_{2.5}$ in northern Chinese cities: implications for policy. Atmos. Chem. Phys. 23, 9455–9471.